

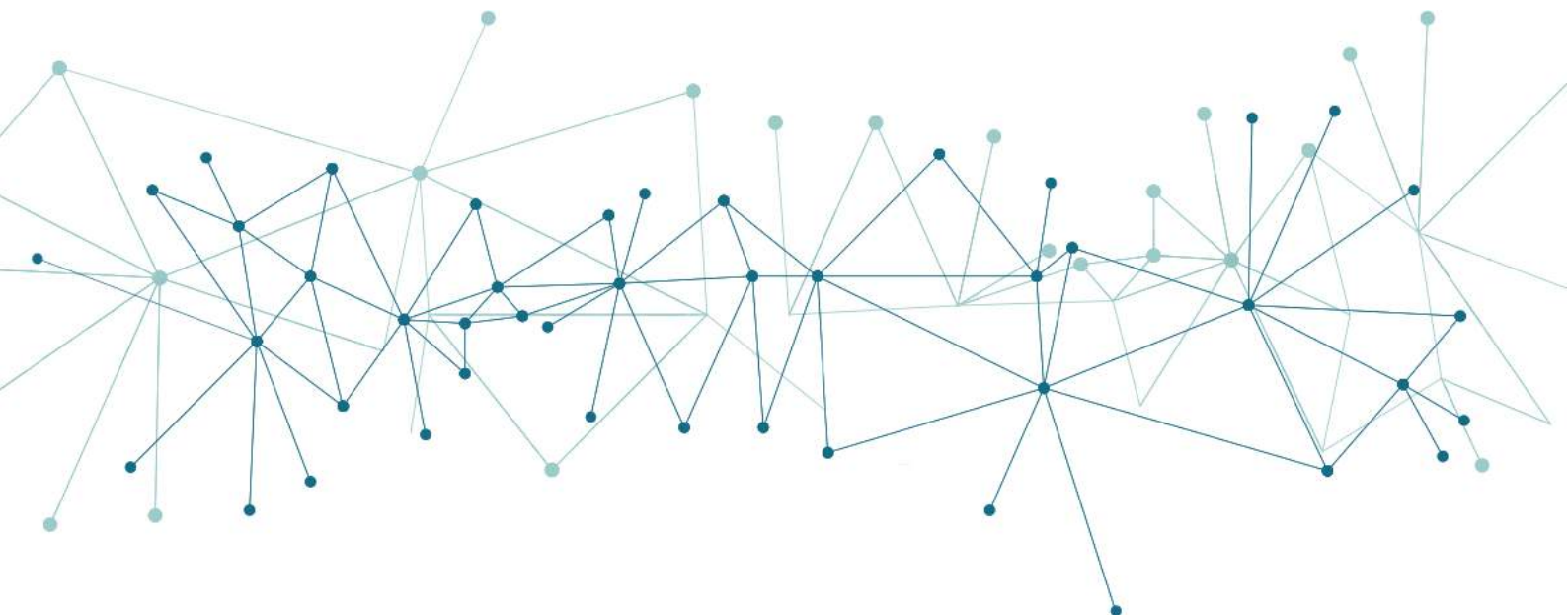


The eDREAM project is co-funded by the EU's Horizon 2020 innovation programme
under grant agreement No 774478



Deliverable: D3.4 – Aerial 3D models and simulation procedures for DR estimation V1

Lead Author: Charalampos Psarros (TU)



Imprint

Aerial 3D models and simulation procedures for DR estimation V1, May, 2019

Contractual Date of Delivery to the EC:	31.05.2019
Actual Date of Delivery to the EC:	31.05.2019
Author(s):	Charalampos Psarros, Benjamin Hunter (TU) Joao Patacas, Fathi Abugchem (TU) Giorgos Sfikas (CERTH) Mircea Bucur (KiWI)
Participant(s):	Leader: TU Contributing partners: CERTH, KiWI
Project:	enabling new Demand Response Advanced, Market oriented and secure technologies, solutions and business models (eDREAM)
Work package:	WP 3 – Techniques for DR and Energy Flexibility Assessment
Task:	T3.4 – Aerial Survey techniques for DR potential estimation
Confidentiality:	public
Version:	1.0

Legal Disclaimer

The project enabling new Demand Response Advanced, Market oriented and secure technologies, solutions and business models (eDREAM) has received funding from the European Union's Horizon 2020 research and innovation programme under grant agreement No 774478. The sole responsibility for the content of this publication lies with the authors. It does not necessarily reflect the opinion of the Innovation and Networks Executive Agency (INEA) or the European Commission (EC). INEA or the EC are not responsible for any use that may be made of the information contained therein.

Executive Summary

This document presents information regarding preparatory work towards development of aerial 3D models and simulation procedures for DR estimation. It is the first of two deliverables (D3.4 and D3.8) comprising task T3.4. D3.4 contains the preparatory work and research towards the task providing the necessary groundwork for data collection and processing to happen in D3.8.

The document summarises technical specifications and requirements regarding the hardware and software to be used, including considerations for a range of options for drones, sensing equipment and relevant software. Aerial Survey techniques are also mentioned, relevant to the options available to us through the software and hardware considered for the task.

Challenges regarding the original Aerial Survey pilot site's location are mentioned and explained, including description and explanation on suitability regarding alternative pilot site chosen.

Finally, image processing and modelling techniques are described and illustrated regarding the data collected and the processes to be applied on thermography, visible spectrum and laser scanned (LiDAR) data.

Table of Contents

1	Introduction	7
1.1	Scope and objectives of the deliverable	7
1.2	Structure of the deliverable	7
1.3	Relation to other tasks and deliverables.....	8
1.4	Methodology.....	8
2	Technical specifications and development	9
2.1	Drone considerations	9
2.1.1	Models/capability, requirements.....	9
2.1.2	Navigation options/specs, considerations	14
2.2	Payloads	16
2.2.1	LiDAR.....	16
3	Software	23
3.1	LiDAR	23
3.2	Thermography.....	23
3.3	Photogrammetry.....	25
3.4	Alternative considerations	26
4	Aerial Survey.....	27
4.1	Site considerations, suitability	27
4.2	3D scanning (TU)	29
4.3	Image and data acquisition	30
5	Data Analysis and DR estimation	33
5.1	Image Processing (TU, CERTH)	33
5.2	Modelling of surveyed area and energy performance estimation.....	39
5.2.1	Comparison of data/results with current industry standard procedures	41
6	Conclusions.....	44
	References	46
	ANNEX: Title of Annex	Error! Bookmark not defined.

List of Figures

Figure 1	IP Ratings: first characteristic numeral definitions	11
Figure 2	IP Ratings: first characteristic numeral definitions	12
Figure 3	Flight times in relation to payload weight (Heliguy.com)	13
Figure 4	RTK system (Heliguy.com)	15
Figure 5	Velodyne LiDAR puck connection box modeified with U-Blox Neo 6M GNSS module	18
Figure 6	Velodyne LiDAR puck connection box modeified with U-Blox Neo 6M GNSS module	18
Figure 7	Velodyne LiDAR puck connection box modeified with U-Blox Neo 6M GNSS module	19
Figure 8	Velodyne LiDAR puck connection box modeified with U-Blox Neo 6M GNSS module	19
Figure 9	Velodyne LiDAR puck connection box modified with U-Blox Neo 6M GNSS module	20
Figure 10	Vertical scanning LiDAR mount assembly	21

Figure 11 3D printed prototype horizontal LiDAR mount, attached to drone single gimbal mount	21
Figure 12 FLIR Tools software	23
Figure 13 FLIR Tools interface	24
Figure 14 FLIR Tools interface showing thermography parameters.....	24
Figure 15 Exported CSV file showing individual per-pixel temperature values	25
Figure 16 R158 Restriction Zone where Moore House is located.....	27
Figure 17 Ernest Dence Estate area	28
Figure 18 Google 3D aerial view of UK pilot site (Ernest Dence estate, Greenwich, London).....	30
Figure 19 Pix4DCapture mission planning User Interface	30
Figure 20 Example image (left) and semantic segmentation map (right). The semantic segmentation map is pseudocolored, with each colour corresponding to a semantic category (here, blue = ROI/building, yellow = sky, etc.).	35
Figure 21 A pretrained convolutional neural network can be used in a non-standard manner as a feature extractor: Such features (as the “hypercolumns” introduced by [Hariharan2015]) may then be used in the context of an unsupervised method.....	37
Figure 22 Outline of the pipeline envisaged for the manual annotation / model training component of the image processing module.....	37
Figure 23 Outline of the pipeline envisaged for thermal loss index estimation.	38
Figure 24 Energy performance assessment based on SEMANCO project – adapted from Dawood et al. (2017) ...	41
Figure 25 Determination of Energy demand reduction potential using EPC – adapted from OFGEM (2017).....	43

List of Acronyms and abbreviations

eDREAM	enabling new Demand Response Advanced, Market oriented and secure technologies, solutions and business models
BEPS	Building Energy Performance Simulator
CAA	Civil Aviation Authority
CAP	Civil Aviation Publication
CSV	Comma Separated Values
DR	Demand Response
EHCS	English House Condition Survey
EMF	ElectroMagnetic Field
FoV	Field Of View
GNSS	Global Navigation Satellite System
GPS	Global Positioning System
GPU	Graphics Processing Unit
GSD	Ground Sampling Distance
HEED	Homes Energy Efficiency Database
IP rating	Ingress Protection rating
IR	InfraRed
LiDAR	Light Detection And Ranging
ONS	Office of National Statistics
RDSAP	Reduced Data Standard Assessment Procedure
RF	Radio Frequency
RGB	Red Green Blue
ROI	Region Of Interest
RTK	Real-Time Kinematic
SAP	Standard Assessment Procedure
UAV	Unmanned Aerial Vehicle

1 Introduction

1.1 Scope and objectives of the deliverable

This deliverable's objective is to report methods for application of drone aerial survey technology to estimate demand response over a wide area of surveyed building assets.

1.2 Structure of the deliverable

Deliverable 3.4 is structured into 5 chapters, each with their corresponding subchapters.

Chapter 1 is an introduction to the deliverable, explaining the scope, objectives and structure of the deliverable

Chapter 2 includes the technical specifications of the deliverable. It describes the different technologies considered regarding the drone and the payloads being used to gather the data. Different types of drones are considered and outlined with each advantages thoroughly described. Same for payloads, the different available cameras and LiDAR scanners are being outlined, describing the preferred specifications leading to the models selected to carry through this task.

Chapter 3 includes an overview of the software used for the task. It describes the different software used for thermography, photogrammetry and laser scanning using LiDAR equipment. It also includes alternative experimental considerations to the mentioned methods, such as videogrammetry.

Chapter 4 is focussed on the processes regarding the Aerial Survey. It explains the test site considerations and relevant regulations, 3D scanning methods and data acquisition methods in order to get models based on data acquired from visible/thermography and laser scanning sensors.

Chapter 5 includes an analysis of the image processing techniques used to process the acquired data. It includes processes of both visual and thermography imagery in order to calculate thermal loss index estimation and also detect ROI (Regions of Interest).

1.3 Relation to other tasks and deliverables

Deliverable D3.4 refers to the task 3.4 of WP3 and presents preparatory work towards development of aerial 3D models and simulation procedures for DR estimation. This part reports on the first version of models and techniques identified for the application of drone aerial survey technology to estimate demand response potential over a wide area of surveyed building assets. The relevant local regulations of drone aerial survey at chosen pilot site were reported on WP2 deliverable D2.3.

The final part of task 3.4 consists of D3.8 and will take care of the actual development of aerial survey toolkit based on the methods and techniques reported in this deliverable. Deliverable D3.8 will validate and provide accuracy comparison between various aerial survey techniques and modelling methods.

The goal of task 3.4 and hence deliverable D3.4 and D3.8 is to identify peak and minimum energy demand requirements of the assets using a drone equipped with HD optical, thermal imaging and LiDAR scanners. Data collected by the drone will help determine estimates of aggregated and individual extremes of energy demand of assets. The outcomes of the collected data will feed into other work packages within eDREAM project mainly Baseline Flexibility Estimation component of WP3 task T3.2.

1.4 Methodology

Production of this document is predominantly a result of desktop research applied to collect and analyse information from various published information sources. Recommendations and justifications for many decisions made in this task are presented in this document, such as software and hardware tools chosen. This document also reports the development process of a custom mounting solution, as well as power and data logging solutions to adapt a Velodyne LiDAR unit for use in aerial survey activities, attached to a drone and operating independently of ground equipment.

2 Technical specifications and development

2.1 Drone considerations

Aerial survey techniques required the use of a drone, therefore appropriate equipment had to be considered and acquired.

Initially, in-house development of a custom drone was briefly considered, however a decision against it was made for reliability and compliance reasons. Following research on the market, a widely used brand was chosen (dji) and their various offerings were considered. Our department already owns equipment by dji (Phantom 3 Advanced, custom-fitted with a thermal camera), however, this was deemed unsuitable for our needs mainly due to its inability to carry required payloads of certain weight. Payloads will be discussed further within this document.

2.1.1 Models/capability, requirements

Dji is a widely used drone manufacturer, offering a variety of drones and accessories aimed at a range of target markets, from hobbyists and prosumers to professionals to industrial users.

Their more portable hobbyist and prosumer ranges (Spark, Mavic, Phantom series), while looked upon in an attempt to optimise costs, were deemed unsuitable due to inability of adequately carrying payloads of certain weight as previously mentioned.

There are two model series available that are able to carry payloads such as dji's own gimbals/cameras or potential custom devices, the Inspire and the Matrice series.

The Inspire 2 model was considered as well as the Matrice 200 and 600 series, being the models aimed for enterprise/industrial use. All three series share the same mounts accepting dji's gimbal/camera modules and offer capabilities of flying with custom payloads. Inspire2 was quickly ruled out due to its limited payload capacity (less than 1kg). Furthermore, the more industrial/enterprise targetted Matrice series were also capable of longer flight times and were of overall more robust construction allowing them to be flown during more severe weather conditions.

Having to choose between M200 and M600 series, the M600 model was quickly ruled out for a number of reasons. One of the reasons was compliance. M600 is a hexacopter (uses 6 motors/propellers) as opposed to the other quadcopter (4 motors/propellers) drones, requiring 6 batteries to fly and making it a rather big and heavy drone. Flying

an M600 fully equipped with our intended payloads brings the aircraft in excess of 7kg takeoff weight, subjecting us to further CAA rules and regulations with additional rules applying to such heavier type of aircraft, making operations less flexible. Overall size of the model and battery requirements makes such an aircraft more tedious to operate and maintain, requiring more space and a much higher number of batteries. With a requirement of 6 batteries used for each mission, having an extra two sets of batteries for redundancy and more demanding mission would require a minimum of 18 batteries appropriately maintained and conditioned at all times. Such an endeavour also increases costs exponentially, something undesirable since we need to stick to the project's budget.

M200 series consist of three models, the M200, M210 and M210 RTK. They are largely based on the same quadcopter (M200) with the M210 models adding dual gimbal/payload functionality. M210 RTK offers RTK (Real-Time Kinematic) positioning, a technology explained further in this document.

All three M200 series models offer IP43 weatherproofing. IP ratings means Ingress Protection rating, as defined by international standard IEC 60529, classifying the degrees of protection provided against the intrusion of solid objects/dust and water/moisture in electrical enclosures. IP rating consist of the IP code at start, followed by first characteristic numeral (solids), followed by second characteristic numeral (water). There can also be two optional additional/supplementary letters but the most commonly used format is IPXX with XX comprising the first and second characteristic numeral. The following tables explain the levels of ingress protection for each characteristic numeral.








Degrees of protection against solid foreign objects indicated by the first characteristic numeral			
First characteristic numeral		Degree of protection	
		Brief description	Definition
0		Non-protected	–
1		Protected against solid foreign objects of 50 mm diameter and greater	The object probe, sphere of 50 mm diameter, shall not fully penetrate ¹⁾
2		Protected against solid foreign objects of 12.5 mm diameter and greater	The object probe, sphere of 12.5 mm diameter, shall not fully penetrate ¹⁾
3		Protected against solid foreign objects of 2.5 mm diameter and greater	The object probe of 2.5 mm diameter shall not penetrate at all ¹⁾
4		Protected against solid foreign objects of 1 mm diameter and greater	The object probe of 1 mm diameter shall not penetrate at all ¹⁾
5		Dust-protected	Ingress of dust is not totally prevented, but dust shall not penetrate in a quantity to interfere with satisfactory operation of the apparatus or to impair safety
6		Dust-tight	No ingress of dust

Figure 1 IP Ratings: first characteristic numeral definitions

Degrees of protection against water indicated by the second characteristic numeral			
Second characteristic numeral		Degree of protection	
		Brief description	Definition
0		Non-protected	–
1		Protected against vertically falling water drops	Vertically falling drops shall have no harmful effects
2		Protected against vertically falling water drops when enclosure tilted up to 15°	Vertically falling drops shall have no harmful effects when the enclosure is tilted at any angle up to 15° on either side of the vertical
3		Protected against spraying water	Water sprayed at an angle up to 60° on either side of the vertical shall have no harmful effects
4		Protected against splashing water	Water splashed against the enclosure from any direction shall have no harmful effects
5		Protected against water jets	Water projected in jets against the enclosure from any direction shall have no harmful effects
6		Protected against powerful water jets	Water projected in powerful jets against the enclosure from any direction shall have no harmful effects
7		Protected against the effects of temporary immersion in water	Ingress of water in quantities causing harmful effects shall not be possible when the enclosure is temporarily immersed in water under standardized conditions of pressure and time
8		Protected against the effects of continuous immersion in water	Ingress of water in quantities causing harmful effects shall not be possible when the enclosure is continuously immersed in water under conditions which shall be agreed between manufacturer and user but which are more severe than for numeral 7

Figure 2 IP Ratings: first characteristic numeral definitions

IP43 rating for the M200 series means it is protected for intrusion solids of 1mm or grater and also against spraying water at and angle up to 60° on either side of the vertical. That makes the drone technically suitable to fly it even in rain conditions, provided wind speeds are still within spec.

Another reason the M200 series were considered were the adequately long flight times under various payload weight configurations. The following table illustrates flight times using both normal (TB50) and higher capacity (TB55) configurations under several payload scenarios. DJI gimbal/camera models have been used as examples, plotted across the various payload weights within the graph. All M200 series drones also come with a maximum 2kg payload with the RTK model having reduced capacity due to the need of extra antennas adding to the overall weight.

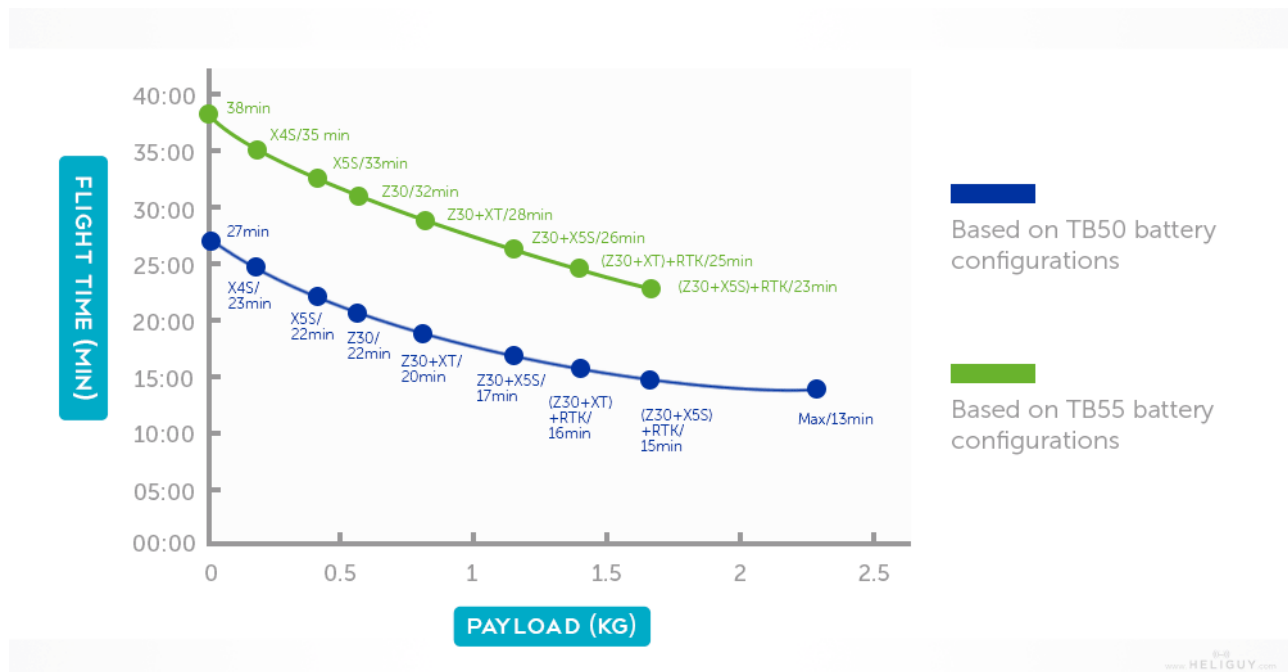


Figure 3 Flight times in relation to payload weight (Heliguy.com)

Considering the versatility of dual gimbal/payload functionality, the dji Matrice M210 drone was chosen. M210 comes in two variants, M210 and M210 RTK. The difference is explained within the next section.

2.1.2 Navigation options/specs, considerations

Having concluded on M210 as the drone model to be used, two options were available, M210 and M210 RTK. Both models use a combination of global navigation satellite systems (GNSS) such as GPS and GLONASS (or GPS and BeiDou when used in China) for positioning and navigation. What M210 RTK uses in addition is a ground station to achieve RTK results.

RTK stands for Real-Time Kinematic. It is a positioning system that offers pinpoint precise (centimetre-level) accuracy alongside robustness against scenarios involving RF (Radio Frequency) and EMF (ElectroMagnetic Field) interference, factors that can affect satellite-based positioning (GPS/GLONASS/BeiDou) signals. It works by combining satellite positioning signals with the ground station.

The RTK system has additional antennas in order to communicate with a ground station based on a fixed position. It combines the satellite based positioning with that of the ground station in order to achieve the desired specified precision. The following image illustrates how a typical RTK equipped drone functions.

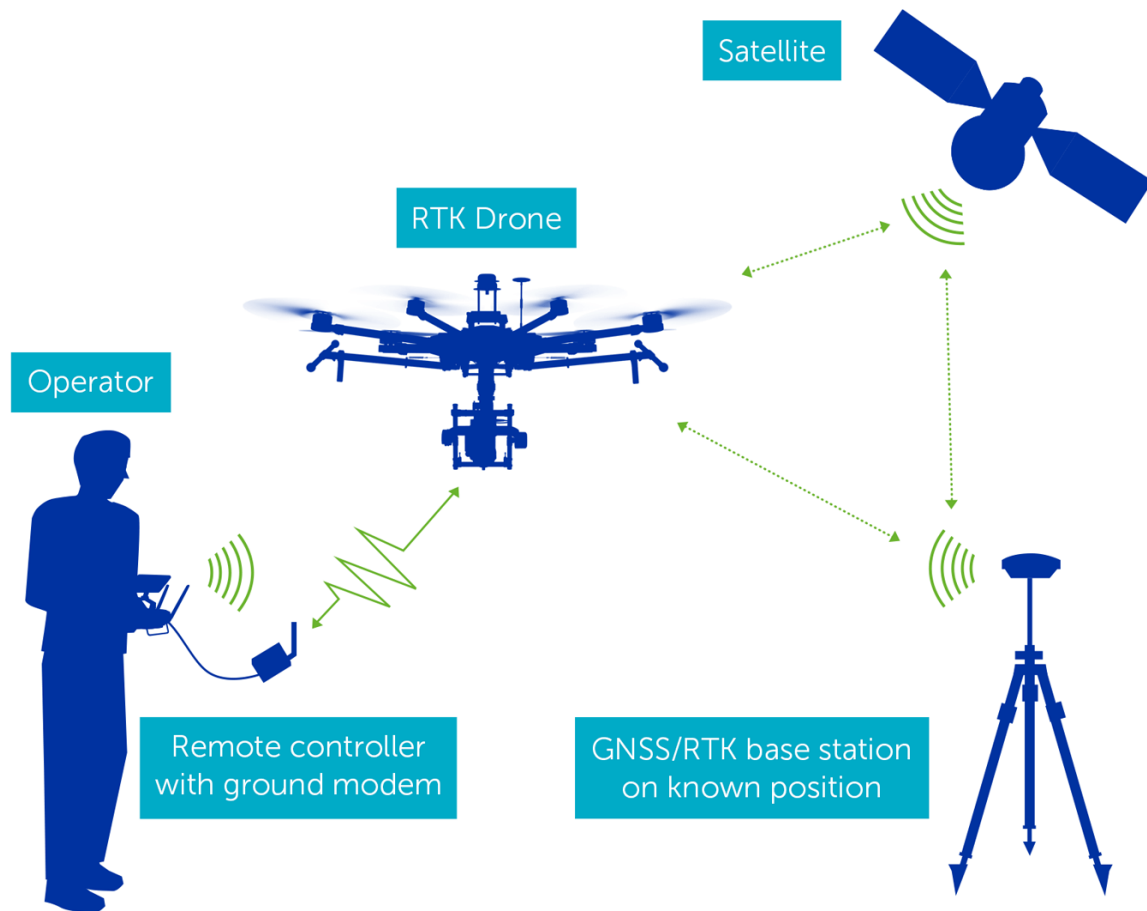


Figure 4 RTK system (Heliguy.com)

RTK is ideal in cases where inspections need to take place at locations with high interference such as power lines, telecommunication installations or offshore rigs. For the purposes of this task, the non RTK model is adequate, in fact more appropriate, considering several inconveniences it adds to the process. For example whenever the ground station is moved (i.e. drone out of sight/other side of building with signals blocked), the system must be updated and such a procedure is not possible when the aircraft is flying. The extra antennas also add to the overall weight of the system, negatively affecting the drone's payload capacity and total flight time.

Considering the extra complexity setting up, negative effects on payload and also the extra cost RTK functionality adds, it was concluded that the non RTK model will be used for the purposes of this task

2.2 Payloads

A payload is due to the various sensors and relevant devices we attach to the drone in order to do the aerial survey and collect the desired data. For the purposes of this task, cameras will be used (operating using both visible light and thermal imaging) as well as a LiDAR (Light Detection And Ranging) laser scanning device including its supporting electronics for power, processing and communication purposes. It is the most important element of this task as it is the part that will be used to collect the data, the drone merely being a vehicle helping us to get our sensors/equipment to required locations.

2.2.1 LiDAR

Teesside University has a Velodyne 'Puck' VLP-16 Real-Time 3D LiDAR system. This is a 16-laser scanning system (903nm narrow band infrared wavelength) of compact dimensions, and has a 100m range and a scan rate of about 300.000 points/sec, accuracy of +/- 3cm (typical), up to a 360° horizontal and 30° vertical field of view with +/- 15° up and down. The unit weighs 830grams and has a low power consumption of 8w, making it suitable to be part of a payload, allowing us to add up to 1170g in support systems/electronics for a total of 2kg max payload as specified by the aircraft manufacturer, DJI.



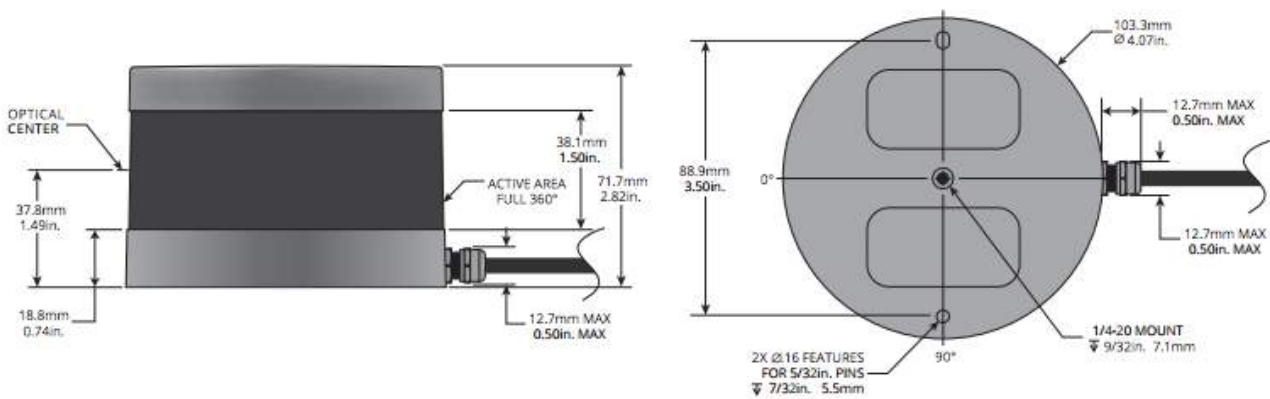


Figure 5 Velodyne VLP-16 LIDAR and dimensions (Velodyne.com)

One consideration that should be made is that VLP-16 was primarily designed by Velodyne for deployment in automotive and ground-based robotic applications, and therefore relies on a connection to a DC power source and an Ethernet network for power and data communications. As such, some development effort was required to adapt this unit for use onboard a Drone.

As the electrical power requirements of the LiDAR unit are very small relative to the aircraft's propulsion systems, it was determined that running the LiDAR from the aircraft's battery resulted in an insignificant change to flight times. Because of this it was decided to power the LiDAR from the aircraft's onboard battery via the Power takeoff port. Although the voltage of the aircraft's power output is appropriate for the LiDAR unit, good practise dictates that there should be a switch and some over-current protection inline. This will be incorporated into a PCB, which will be constructed to accommodate LiDAR and data capture connectivity.

In this application, it is important to have GNSS functionality for both accurate timing information and geolocation for accurate referencing of points in the point cloud produced. The VLP-16 does not come with this functionality as standard and there are two options for adding it. Firstly, a consumer grade Garmin unit with custom firmware can be purchased from Velodyne and plugged into the connection box. This proved difficult to source, and as the connection box was going to be replaced anyway the second option was chosen, which was to add a custom GNSS unit, configured to output specific messages that the LiDAR can understand. During early prototyping this was added to the LiDAR connection box, however in subsequent revisions it will be added to the PCB which will be constructed to handle connectivity and power management. The modified LiDAR connection box is shown below in Fig 5.



Figure 5 Velodyne LiDAR puck connection box modified with U-Blox Neo 6M GNSS module

For data logging a piece of computer hardware is required to capture and store the UDP packets broadcasted over the LiDAR's Ethernet port. An Intel Atom based miniature PC was chosen to perform communication and data capture activities. This is connected to the LiDAR using a USB Ethernet adapter, and communication with the PC is performed over built in 802.11ac WiFi. This PC requires a 5V DC power supply, and therefore a step-down DC-DC converter will be included in the LiDAR PCB.

The specifications of the PC chosen is shown in Fig. 6, the dimensions of the device are shown in Fig 7 and the functional diagram of the LiDAR power and data capture assembly is shown below in Fig 8.

CPU	Intel Atom X5 Z8350 (4 core, 1.44GHz base, 1.92GHz boost)
GPU	Intel integrated
RAM	4GB DDR3L-1333
Cooling	Active (fan cooled aluminium heatsink)
WLAN	802.11 a/b/g/n/ac, 2.4Ghz & 5.0Ghz
Bluetooth	4.0
Rated CPU TDP	2w
PSU requirements	5v USB Micro-B up to 3A
Weight	50g
Dimensions (mm)	120 x 38 x 13
USB	1x Type A 2.0, 1x Type A 3.0,
eMMC	64GB
Expandable storage	Micro SDXC (up to 128GB supported)

Figure 6 Velodyne LiDAR puck connection box modified with U-Blox Neo 6M GNSS module

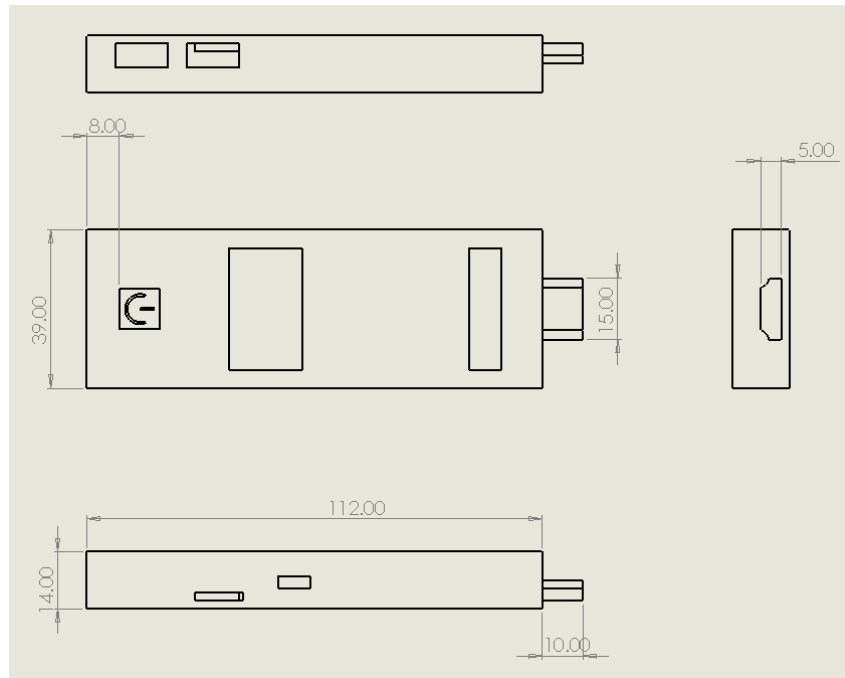


Figure 7 Velodyne LiDAR puck connection box modified with U-Blox Neo 6M GNSS module

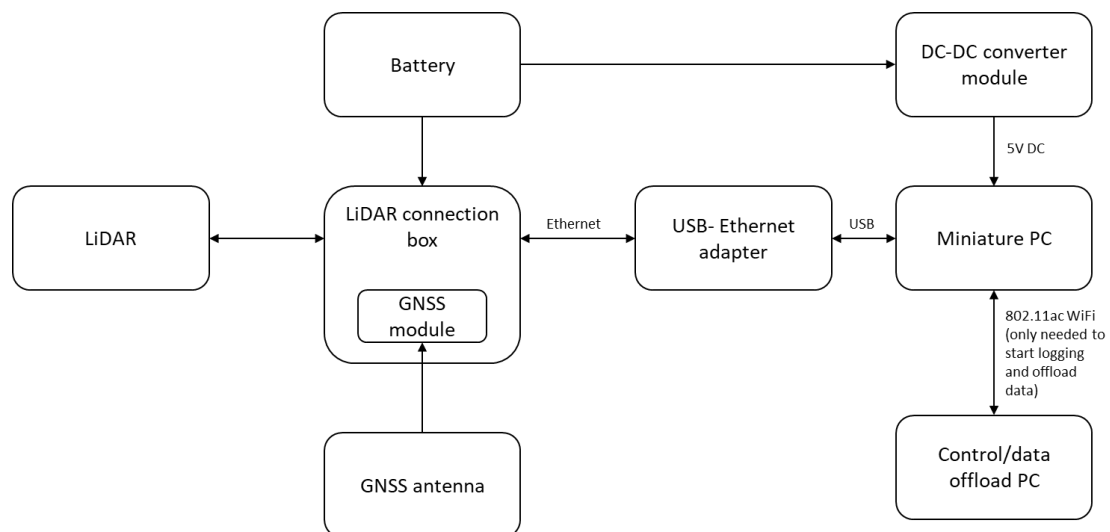


Figure 8 Velodyne LiDAR puck connection box modified with U-Blox Neo 6M GNSS module

For physical mounting, the LiDAR unit has a centrally located $\frac{1}{4}$ " UNC thread mounting screw hole on the base, accompanied by two locating dowel holes to prevent the LiDAR unit from turning. This is illustrated in (LiDAR drawing figure) In order to securely mount this device to an aircraft a custom mounting system must be designed and produced to interface between the DJI Skyport gimbal connector and the base of the LiDAR unit, with the flexibility to adjust the angle of the LiDAR for optimal scanning performance. To deal with this problem, 3 parts were constructed; A DJI Skyport to hinge adapter, a horizontal scanning LiDAR mount and vertical scanning LiDAR mount. These are illustrated below in XX, along with a 3D printed prototype horizontal mount in Fig. 9.

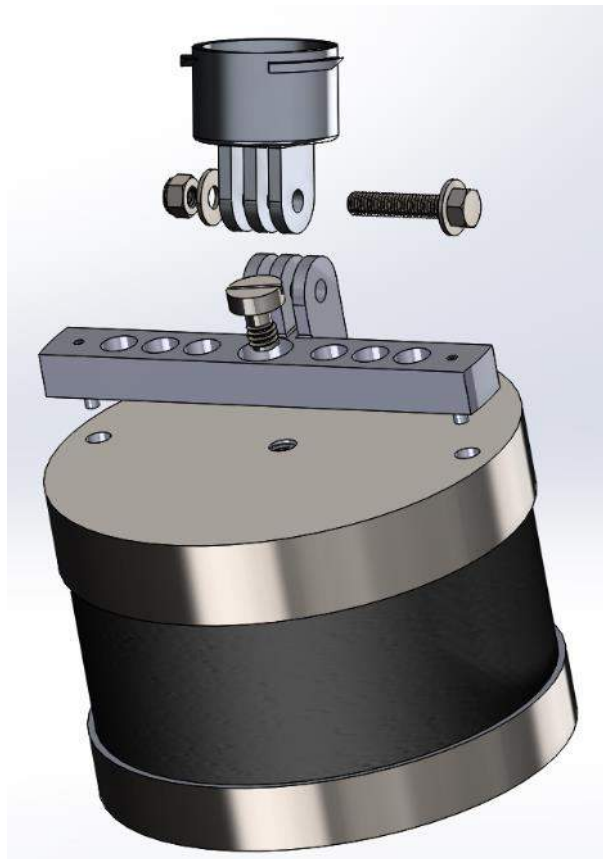


Figure 9 Velodyne LiDAR puck connection box modified with U-Blox Neo 6M GNSS module

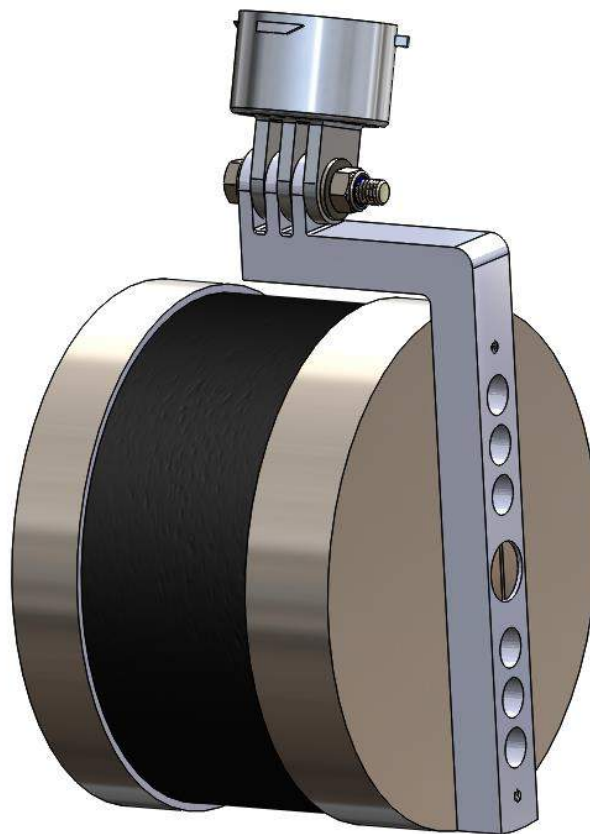


Figure 10 Vertical scanning LiDAR mount assembly



Figure 11 3D printed prototype horizontal LiDAR mount, attached to drone single gimbal mount

2.2.2 Cameras

For simplicity, absolute compatibility and reliability, dji camera (Zenmuse) payloads have been chosen. There are three visual light cameras compatible with the Matrice M210 drone: Zenmuse Z30 Zoom, X5S and X4S.

Zenmuse Z30 Zoom is dji's most powerful aerial zoom lens, offering a maximum of 30x optical zoom factor and 6x digital zoom that can result in a total magnification of up to 180x, ideal for situations where you need to keep a rather long distance away from the subject. The resolution of the captured footage is 1920x1080pixels at 30 frames per second.

Zenmuse X5S is able to shoot video at 4K resolution at 60 frames per second and 20.8Megapixel stills.

Zenmuse X4S is a 20Megapixel resolution camera with an 1-inch CMOS sensor and a max sensitivity of 12800 ISO, making it a good camera for low light and detailed work. It is capable of shooting 4K resolution video at 60 frames per second.

Matrice M210 is also compatible with two thermal imaging cameras made in collaboration between dji and FLIR, the Zenmuse XT and Zenmuse XT2. The XT is an older model, therefore the XT2 was considered.

Zenmuse XT2 is a dual sensor camera module, featuring both a visual light camera and a thermal imaging sensor. It uses a 1/1.7" CMOS visual sensor and a FLIR Tau 2 Thermal sensor for thermal imaging. It comes in 9 and 30Hz (effectively frames per second) versions and in 9,13,19,25mm focal length versions for the visual sensor. It has an IP rating of IP44.

The visual light sensor records 4K footage at 30 frames per second while the thermal imaging sensor records at 640x512 or 336x256 pixels depending on the model. The 640x512 model has a thermal range of -25° to 135°C while the 336x245 model's range is -25 to 100°C. Overall sensitivity is <50 milliKelvins (mK).

The camera payload chosen for the task was the Zenmuse XT2 because of its ability to capture both thermal and visual images at the same time. The model chosen was the 30Hz version for potential ability to extract features from captured thermal video and the 640x512 model for the extra resolution. The 19mm lens model was chosen for extra detail being more zoomed in. The 25mm model was avoided due to the extra weight it added (629g as opposed to 588g for all other versions).

3 Software

3.1 LiDAR

The basic data output of the Velodyne VLP-16 is performed by means of UDP packets broadcasted over an Ethernet network. The composition of these packets can be found in the unit's user manual and programming guide. The most basic form of data capture for this device would be to capture the packets directly using a program such as Wireshark. These packets may be deconstructed to retrieve LiDAR measurements (azimuth, elevation angle, distance to object and time stamp) and GPS messages (\$GPRMS messages) or fed into other software tools, such as the software provided with the LiDAR unit, VeloView, for calculating spatial X,Y,Z coordinates and then visualising or converting this to other usable formats. VeloView also has baked-in packet capture, and can record while simultaneously parsing the packets, calculating spatial coordinates and visualising LiDAR scan data.

3.2 Thermography

FLIR Tools will be used for acquisition and initial processing of the images (figure 12, 13).



Figure 12 FLIR Tools software

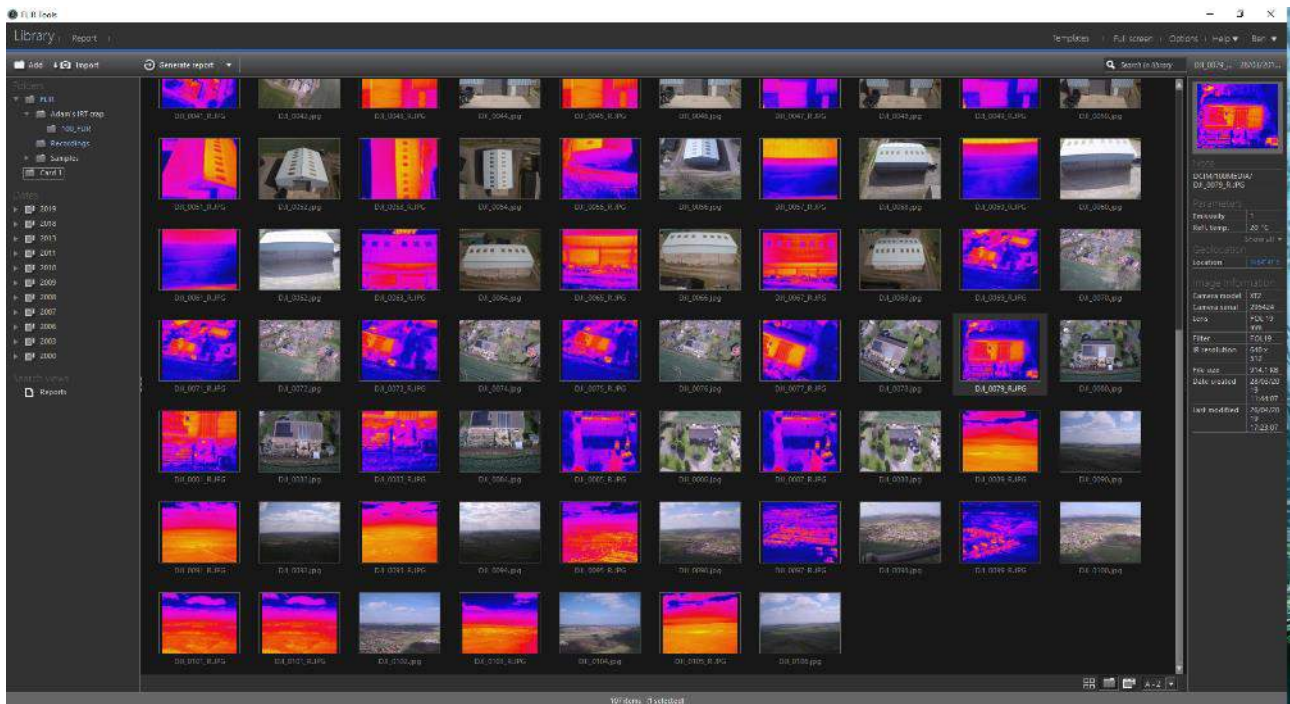


Figure 13 FLIR Tools interface

FLIR tools provide functionality such as reporting of the image's geolocation data provided by the drone's GNSS, colour palette adjustment for the thermograph, spot temperature measurements (using single or multiple locations) and exporting thermography data as a .CSV file containing temperature values for every pixel taken using the thermal camera sensor.

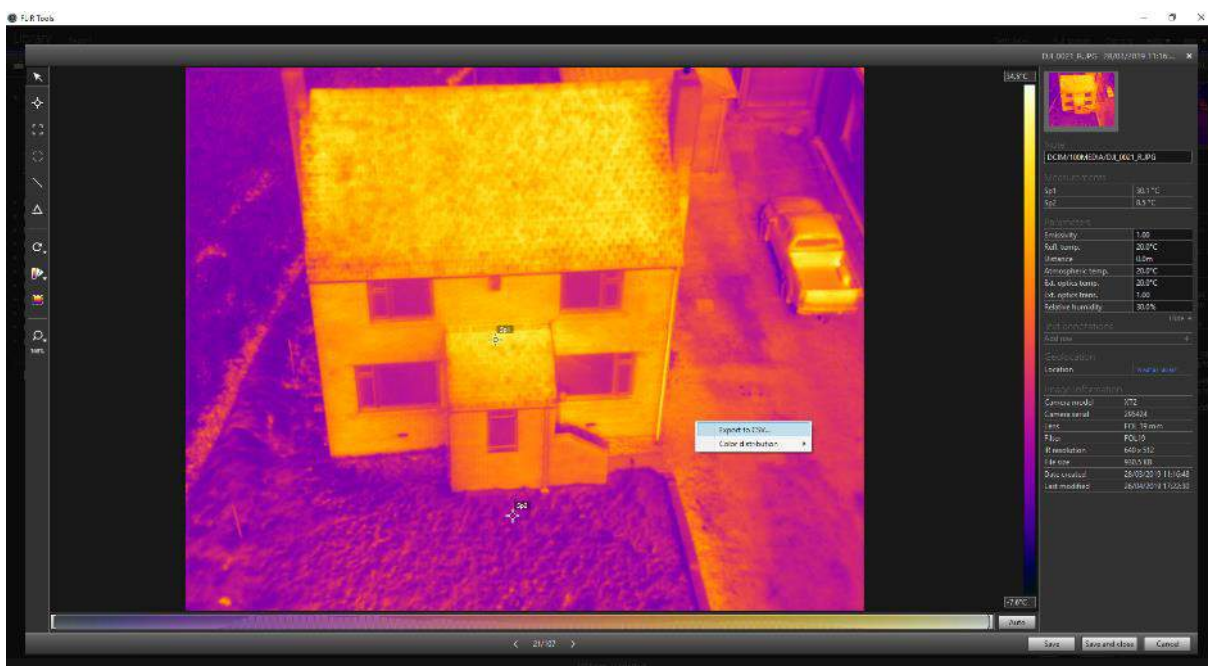


Figure 14 FLIR Tools interface showing thermography parameters

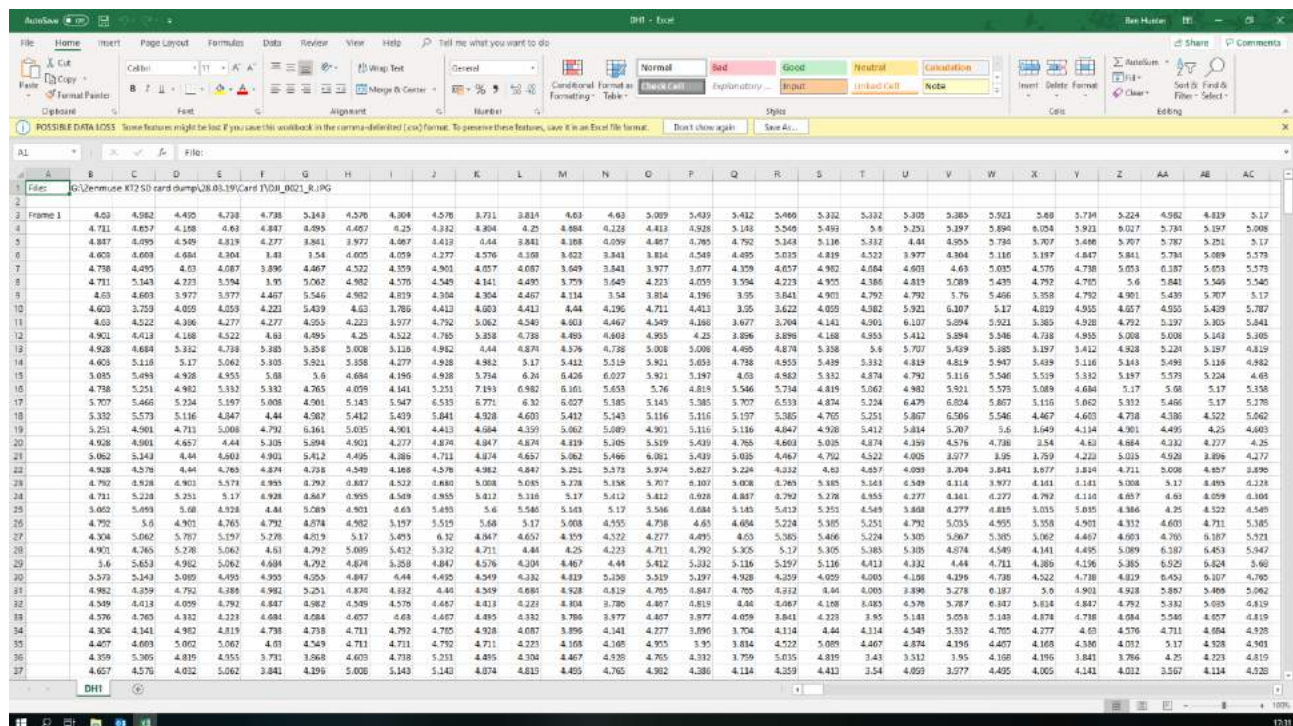


Figure 15 Exported CSV file showing individual per-pixel temperature values

For our use case, it offers functionality of providing appropriate data from imagery, useful for image processing and other automated processes. Details of the image processing stage are described in further detail in chapter 5.1 of this document

3.3 Photogrammetry

Photogrammetry techniques will be used in order to create a digital 3D model of the test site. Pix4D software suite will be used to process the imagery and output the 3D data. Pix4D provides a set of tools for survey planning and data acquisition and processing.

Pix4Dcapture is a drone flight planning app, used to program flight missions and capture data for 3D modelling and mapping.

Pix4Dmodel is used to process RGB imagery and output a digital 3D model using photogrammetry techniques.

Pix4Dmapper is a drone mapping app, combining acquired visual and geolocation data.

Pix4Dmapper and Pix4Dmodel will be used to process the images while a combination of Pix4Dcapture mobile app and DJI's own control software will be used to perform the aerial survey and acquire visual and thermography material.

3.4 Alternative considerations

Alternative methods are also being considered for image acquisition such as videogrammetry. Videogrammetry is similar to photogrammetry, only using a video stream as source material instead of static images, albeit usually of less resolution. Experimental work is ongoing using both normal 360° cameras. The Pix4D suite will also be used for videogrammetry processing.

4 Aerial Survey

4.1 Site considerations, suitability

A building in the City of London has been initially proposed as the demo site for the task. The site was chosen as an interesting use case as most assets were in DR programmes and also conveniently located on the rooftop (6 chillers). KiWi Power also has historical data to document energy consumption and performance in DR programs. However, after investigating the location of the site and considering the relevant regulations and legislation (UK Air Navigation Order CAP 393), it was deemed unsuitable as it is within a no fly zone.

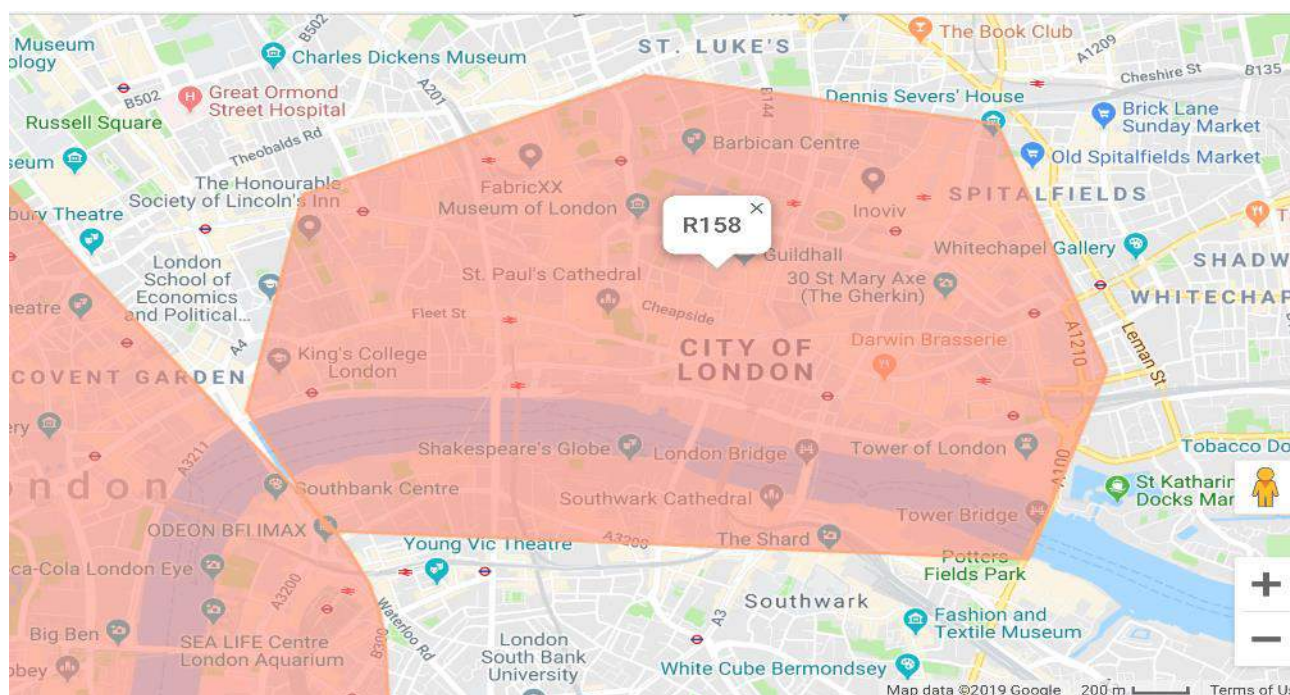


Figure 16 R158 Restriction Zone where Moore House is located

An alternative site was suggested by KiWI power, Ernest Dence Estate at Greenwich. Ernest Dence Estate is a three building complex served by a communal heating scheme where three gas boilers are used for heating and domestic hot water. A number of properties within the building complex have also been fitted with smart metering devices monitoring consumption of electricity as well as indoor temperature. Moreover, there is a working enhanced BEPS (Building Energy Performance Simulator) model developed that can independently be used for assessing various actions such as retrofitting insulations or windows. Ernest Dence estate, contrary to the initially proposed site, is not within a no fly zone.

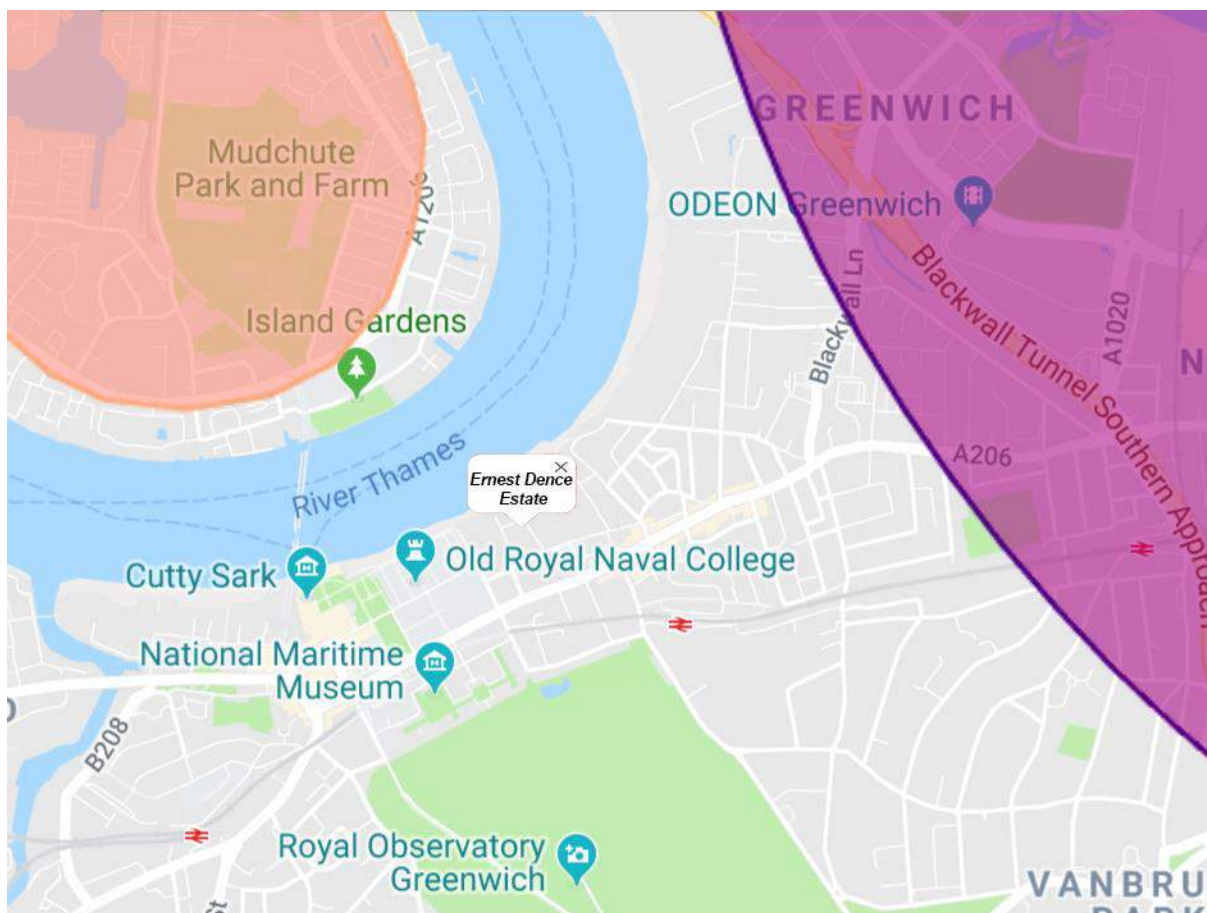


Figure 17 Ernest Dence Estate area

4.2 3D scanning

A Velodyne VLP-16 A significant part of the aerial surveying task consists of scanning the site with a LiDAR unit to gather spatial data required to generate a dimensionally accurate model of the site to be assessed.

Before LiDAR scanning activities can commence, a flight plan must be constructed to ensure that the most appropriate data can be collected, while obeying CAA regulations, ensuring safety and taking into consideration various equipment constraints such as the scanning range and FoV (field of view) of the LiDAR unit. This flight plan can then either be used to guide a manual flight by overlaying the flight path onto a GPS map within DJI's pilot software, or be used to create a mission flight, where the aircraft operates autonomously, following the pre-set route with minimal or no user input. Alternatively, Pix4D capture software may also be used to automatically generate scanning patterns which may be executed automatically. In order to construct a flight plan, the height of the building must first be measured. Simple trigonometry can then be used to calculate the optimal distance from the building and LiDAR mounting angle.

Considerations should also be made regarding whether the whole site should be scanned in a single pass or multiple passes with the LiDAR mount set at different angles for the exterior walls and the roof. Maximum aircraft travel speed should also be carefully considered, as the more slowly a surface is scanned the more measurement points per unit area of building are taken. A target value of points per square meter should be established to ensure that the building is scanned thoroughly enough to avoid missing out important building features. With the consideration of these constraints, the mapping techniques in the following subchapter 4.3 can be applied to perform optimal scanning.



Figure 18 Google 3D aerial view of UK pilot site (Ernest Dence estate, Greenwich, London)

4.3 Image and data acquisition

Image and data acquisition will be done through planned missions and flight paths/patterns while having our visual/thermography equipment as well as the LiDAR attached to the drone.

Pix4D offers the Pix4DCapture companion app that helps plan flight missions for use with their software suite (fig 19)



Figure 19 Pix4DCapture mission planning User Interface

First option is Polygon where it creates a grid style of flight path but within the boundaries of a 2D polygon of which points are defined on the map, aimed to cover the desired area needing to be surveyed. That produces a 2D map and is appropriate for areas which boundaries are not rectangular.

Polygon mode has four parameters: Speed, Angle, Overlap and Face, explained below.

Speed defines the drone's speed and has a range between Fast and Slow. The scale has six levels corresponding to percentages of the max speed between 100% (Fast) and 50% (Slow). The drone's speed ranges between 2m/s and 8m/s and varies during the flight since the drone slows down to take pictures and speeds up again to travel to the next point.

Angle defines the tilt of the camera/sensor between horizontal (0 degrees) and vertical (90 degrees).

Overlap defines the front overlap between 70%, 80% and 90%. The side overlap is calculated so that the side distance between two images is twice the front distance.

Face defines whether the drone should be facing towards the centre of the mission when taking pictures (Center option), or whether the drone should always forward (Forward option).

Second option is Grid, also an option appropriate for 2D mapping. Grid mode is similar to Polygon mode, but the grid flight pattern is generated and flown within rectangular space boundaries. Grid has the same parameters as Polygon: Speed, Angle, Overlap and Face.

Third option is Double Grid. Double grid creates two consecutive nadir grid style flight plan missions within a rectangular boundary area. It is done to ensure taking images from multiple sides including adequate overlap between the imagery. This option is appropriate for 3D mapping. Double Grid has three parameters, Speed, Angle and Overlap.

Fourth option is Circular. This option plans and flies a circular mission around a specified target point with enough overlap required for processing into a model. This option is appropriate for creating models of single objects/buildings. Circular has two parameters, Speed and Capture angle.

Speed is same as within the other modes while Capture angle defines the angle that separates the consecutive images being captured.

Fifth and last option is Free Flight. This option has the drone manually operated by the pilot while the camera shutter is automatically triggered in relation to horizontal and vertical distance intervals. It is useful for complex buildings/structures where polygon is not appropriate/safe enough to use.

A combination of Double Grid, Circular and Free Flight will be used during the testing phase. All three should be appropriate for adequate 3D output and the most efficient one (both time and quality-wise) will be decided during the testing phase and reported within relevant deliverable D3.8.

Visual and Thermography images will be acquired simultaneously while flying the same missions, as our camera has both sensors integrated allowing us for dual capture at both spectrum ranges.

5 Data Analysis and DR estimation

5.1 Image Processing

The data collected by the aerial survey of the audited building is to be used as input to an image processing component. The form of this data is of two recorded modalities: collections of high-resolution, visible spectrum colour images and infrared thermal images, recorded by the UAV for the specific building(s) and at a specific date and time. The goal of the image processing component is to provide an estimate of the building's thermal leakage levels. Thermal leakage for an audit at any given date and time will be computed by the image processing system with respect to the leakage levels of an audit that will be used as the baseline. Thermal leakage levels will be correlated with energy demand requirements, so their estimate becomes useful for in the context of DR estimation. Hence, in the manner described above, peak and minimum demand requirements can be identified for the building, after providing the survey optical/thermal images to the image processing component at different times for the same audited structure.

Both the visible spectrum and infrared modalities are to be used in image processing. The visible spectrum data will be used to identify regions of interest (ROIs) on the structure façade and/or the top plan/roof. This ROI detection step is necessary in order to ignore areas of thermal leakage in the recorded video that are unrelated to the audit. Typical ROIs that may interest us will be windows, doors, chimneys etc. that can be efficiently detected with computer vision techniques. The thermal IR can be used for the detection step to identify false positives.

For ROI detection, we plan to employ two different types of techniques. The first technique will be unsupervised, while the second one will be supervised, in the sense that an annotated dataset will be required in the latter case. We plan implementing the supervised ROI detection technique using deep learning-based methods, inspired by the recent success of such techniques in a wide range of vision tasks [Chen2018, He2017].

Finally, in order to compute the thermal leakage estimate, we will combine the thermal signature data over the ROI estimates and produce a total thermal loss estimate. This thermal loss estimate will be computed as the combined total over partial loss estimates per identified ROI. We expect that the new vision-based technique will be superior to the much simpler drone image post-processing methods used in the literature (thresholding, basic filtering, cf. [Rakha2018, sec.4.3]).

In what follows, we provide details on the two major components of the proposed image processing pipeline: data annotation/ROI detection and thermal loss index estimation. Data annotation and ROI detection

To the end of locating spatial areas that produce strong thermal signature and are at the same time directly related to the building that interests us, thermal IR input is insufficient. Locations with high thermal intensity may appear within the UAV's field of view that may be unrelated to the task at hand (for example, related to a building / construct that does not interest us); if we compute thermal leakage without taking care to include only readings that come from the region of interest, the end-estimate for thermal loss and energy consumption will consequently be higher than its true value.

In order to safely and automatically detect and delineate regions of interest in the drone field of view, it is advantageous to employ the visible range/RGB footage. Semantic-wise, colour images contain a much richer content than thermal IR images. Numerous (RGB-) image-based systems have been proposed in the recent years that are very successful at a wide range of computer vision and image understanding tasks, such as semantic segmentation [Chen2018], instance segmentation [He2017], image classification [Plissiti2018] and object detection [Redmon2016]. The most relevant problems to the task-at-hand are semantic segmentation and salient object detection. Semantic segmentation [Chen2018] involves segmenting an input image into a finite number of spatially and semantically coherent parts or segments, that are at the same time automatically tagged with a semantic label – for example, segment #1 contains a building, segment #2 contains a tree, segment #3 is a generic background class, and so on (see figure. 20 for an example from the bibliography). Salient object detection [Borji2015] involves detecting the one object in the visual input that is semantically the most 'important' – in the context of the current problem, this is the building that we are interested in auditing.



Figure 20 Example image (left) and semantic segmentation map (right). The semantic segmentation map is pseudocolored, with each colour corresponding to a semantic category (here, blue = ROI/building, yellow = sky, etc.).

We plan on tackling the ROI detection problem using two different methods, one unsupervised (no annotated segmentation maps required) and one that is supervised (annotated segmentation maps required for training). These methods will be compared and evaluated on the quality of their output both in qualitative and numerical terms. Numerical evaluation with an objective measure requires annotated ground-truth material [Sfikas2010], that will be the same to be used with the supervised method (after taking into account and partitioning the set into appropriate cross-validation folds). Data annotation is hence a task that can be demanding and time-consuming on its own, especially when a bulk of images need to be semantically annotated. In Figure 20, an example image with its annotation, with the form of the latter as a semantic pixel-level segmentation map is shown. The goal of semantic segmentation system would, after being fed with batches of pairs of images and annotations, to recreate a segmentation map for an ‘unseen’ image (unseen in the sense of not belonging to the training set).

The unsupervised method will use cues and models from the standard arsenal of image processing and computer vision, that may include raw colour information, edge-detection cues and Gabor filters, and likewise standard detection methods such as the Hough transform [Gonzalez2018, Klette2014]. Depth estimates computed using stereo will also provide an important cue, as building façade points should be expected to lie on spatial points that are close to one another, especially compared to 3D signatures of other objects. Depth estimation with stereo is possible with structure from motion techniques, taking advantage of at least two images captured from a close distance to each other (Klette, 2014). In the current context, a stereo-based technique is an option, since the UAV will deliver a multitude of consecutive RGB frames of the target building. Other, more recently proposed cues may be considered, such as Quaternionic Gabor

filter banks (Subakan2011) that can capture Fourier spectrum-based features on multimodal images.

Furthermore, we plan on employing an unsupervised learning scheme to group the aforementioned low-level features and perform the desired image segmentation. With respect to segmentation methods, the efficiency of standard methods may be investigated, such as using k-means to cluster pixel-level cues, or modelling these latter as a Gaussian Mixture Model (Sfikas 2008). Other well-known methods for segmentation include normalized cuts (Shi 2000), which treats segmentation with an elegant graph-theoretic approach; segmentation in superpixels segments the image first into spatially coherent groups of pixels ('superpixels') (Achanta 2012), and can be performed as a preprocessing step before applying a second method to group superpixels into larger segments, as for example in (Sfikas 2011). Simple Iterative Linear Clustering is a simple and fast, yet powerful superpixel creation method (Achanta 2012, Ren 2015). Segmentation using unimodality tests is also a method that we may consider to explore (Chamalis 2017).

With regard to the supervised technique, a deep, fully convolutional network-based method is envisaged, akin to the celebrated Unet and DeepLab architectures (Chen 2015). The result of the technique will be directly a pixel-level semantic segmentation map. Deep learning techniques ideally require GPU-based parallel computations for both training and testing (testing is however considerably less computationally expensive, and can be carried through in a CPU-only environment, albeit at lower speeds), but they typically promise a highly accurate output. On the other hand, supervised techniques carry the risk of having 'overfitted' to the given training set (Retsinas 2018), thus not being practically applicable / non-transferable to data that are sufficiently different to the set over which the training was performed. A third approach, as the middle ground between the two main approaches may be considered: using so-called deep features, or functions of pretrained neural network activations as features with an unsupervised method (figure 21). Aggregations from multiple layers to create fixed-length feature vector in this manner has been recently used and dubbed as 'hypercolumns' [Hariharan2015, Sfikas2016]. Activations from the well-known semantic segmentation network 'Deeplab' [Chen2018] may be considered for this task.

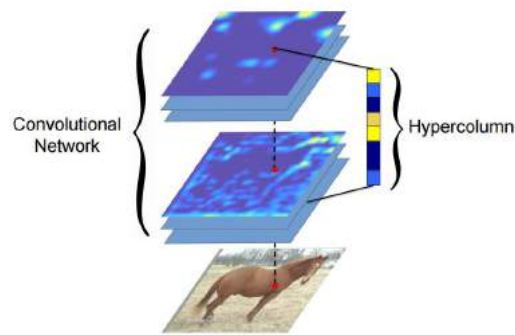


Figure 21 A pretrained convolutional neural network can be used in a non-standard manner as a feature extractor: Such features (as the “hypercolumns” introduced by [Hariharan2015]) may then be used in the context of an unsupervised method.

An outline of the envisaged workflow for data annotation and ROI detection can be examined in figure 22.

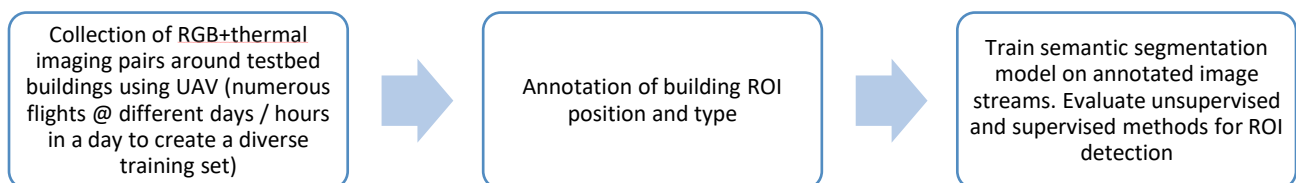


Figure 22 Outline of the pipeline envisaged for the manual annotation / model training component of the image processing module.

After having evaluated and validated the ROI detection methods, these will be used for the next image processing component, which is thermal index estimation per se. The UAV footage will be used to create a 3D point using stereo, by taking into account only region-of-interest points. Furthermore, time-series information will be useful to further segment and track ROIs in time. Time information, along with thermal IR cues, can be used to further refine the segmentation provided by the previous step (in order to, for example, identify and track a specific sub-ROI in the building, such as a window or a door). 3D point information will also be useful to estimate segment area size; this will be combined with the estimated thermal signature distribution using the infrared camera input to output a total thermal loss index per segment.

The aggregate of IR intensities over 3D points for a reading at a specific day and time picked beforehand and arbitrarily will be used as a baseline thermal loss. The thermal loss index for any other day/time will then be defined as the ratio of the IR intensity aggregate compared to that of the baseline. Hence, the thermal loss index for the baseline will by definition be equal to 1. Thermal loss index over 1 will correspond to greater thermal loss, and an index under 1 will correspond to lesser thermal loss.

It is important to stress also that the automatic estimation of thermal loss - either as a relative index, as proposed here, or in absolute energy per unit terms – is a problem that has so far not been discussed by any work in the energy and / or image processing research literature. A work that is perhaps relevant is the recent [Kakillioglu2018], where automated heat leakage detection is discussed, however this is still far from the currently stated objective.

An outline of the envisaged workflow can be examined in fig. 23.

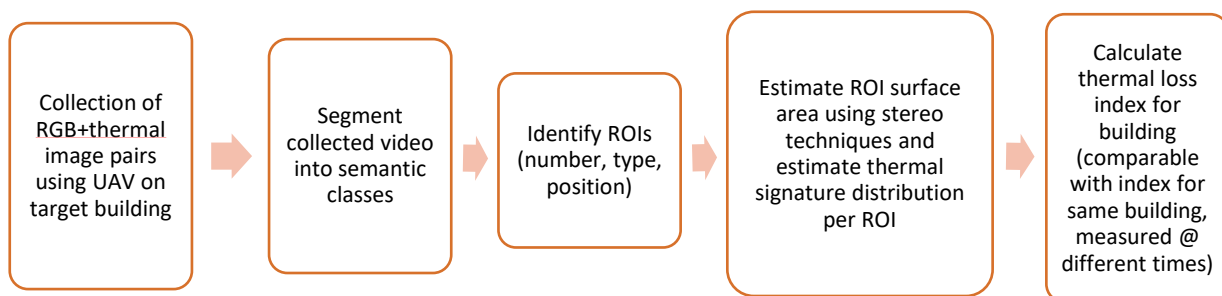


Figure 23 Outline of the pipeline envisaged for thermal loss index estimation.

5.2 Modelling of surveyed area and energy performance estimation

The previously identified UAV surveying methodologies (i.e. using thermal and digital cameras, and LiDAR sensor) will be used to capture the geometric features of building envelopes, and to identify relevant features of buildings and their location (i.e. fenestration and envelope obstructing features) which need to be considered as inputs for the estimation of energy demand.

It is expected that the application of these survey methodologies will provide a high degree of accuracy in the building geometry, which can be used as a basis for the calculation of more accurate estimates of energy demand and identify DR potential in building assets. The UAV survey methodologies will be used to provide improved baseline estimation and improved DR flexibility estimation to increase exploitation potential of building assets in DR programs. In particular, the resulting thermal imagery data will be analysed to provide more detailed information about users/customers behaviour.

UAV surveys can be used to capture the exterior of the existing buildings and surrounding areas, and generate point cloud models using both photogrammetry and LiDAR data-based approaches. In the case of photogrammetry, this can be achieved through the execution of a pre-determined flight plan in which the UAV camera captures a series of photographs. The resulting photographic survey can then be used to build point cloud and mesh models using specialized photogrammetry software (e.g. Pix4D) (Patacas et al. 2018). The resulting 3D models can be used to extract building envelope dimensions, as well as for the identification of building envelope features including the external walls, roof and fenestration areas.

In addition, 3D spatio-thermal models will be developed using photogrammetry by combining the images captured from the UAV's digital and thermal cameras. Since the digital and thermal photos will be taken at the same time according to the pre-determined flight plan, alignment issues between the digital and thermal images will be limited to each of the camera's characteristics, and will be the same for all the captured images. The resulting 3D spatio-thermal model will enable the identification and location of thermal defects and air leakage and provide an assessment of current transmission heat losses, providing important inputs for the assessment of the energy performance of the building (González-Aguilera et al. 2013). The 3D spatio-thermal model can also be used to identify and evaluate defects on the building envelope and identify potential retrofit strategies to improve energy performance (González-Aguilera

et al. 2013; Ham & Golparvar-Fard, 2012). The proposed methodology for the development of 3D spatio-thermal models will enable improved predictions of building energy performance by identifying deviations between actual and expected thermal performance data, providing an improved methodology to assess the energy performance of buildings.

Aerial digital photos and LiDAR data will also be used for the generation of orthomaps that can be used within GIS applications to provide accurate 2D data of the surveyed area. During the digital photo survey, multiple overlapping images are collected as the UAV flies along the pre-determined flight path. The imagery is processed to produce digital elevation data and orthoimage mosaics, named orthomaps. Captured images have perspective geometry that results in distortions that are unique to each image (ESRI 2018). Using Pix4D software, it is possible to process the captured images, so that the resulting image has the geometric integrity of a map. A similar approach can be used to obtain orthomaps from LiDAR data (Gharibi & Habib, 2018).

Once the data resulting from the aerial surveys has been adjusted and properly referenced, it can be converted into GIS and 3D formats such as CityGML (City Geography Markup Language), COLLADA (COLLABorative Design Activity), OBJ, FBX, etc. that are readable within many different standard software packages (Dawood et al. 2017).

Both LiDAR and photogrammetry based models will be used to provide key attributes for the estimation of energy demand, gains and losses of buildings, including accurate envelope & fenestration geometry. The assessment for building energy demand including the inputs and outputs of the process is summarised in Fig 24.

The average ground sampling distance (GSD) will be calculated for the obtained LiDAR and photogrammetry outputs using Pix4D, and will be used as a measure to evaluate their accuracy. The LiDAR, photogrammetry, and ROI approach for thermal images described in section 5.1 will also be compared to evaluate the feasibility of identifying the various building envelope features, including roof, walls, fenestration areas, and building envelope obstructing features.

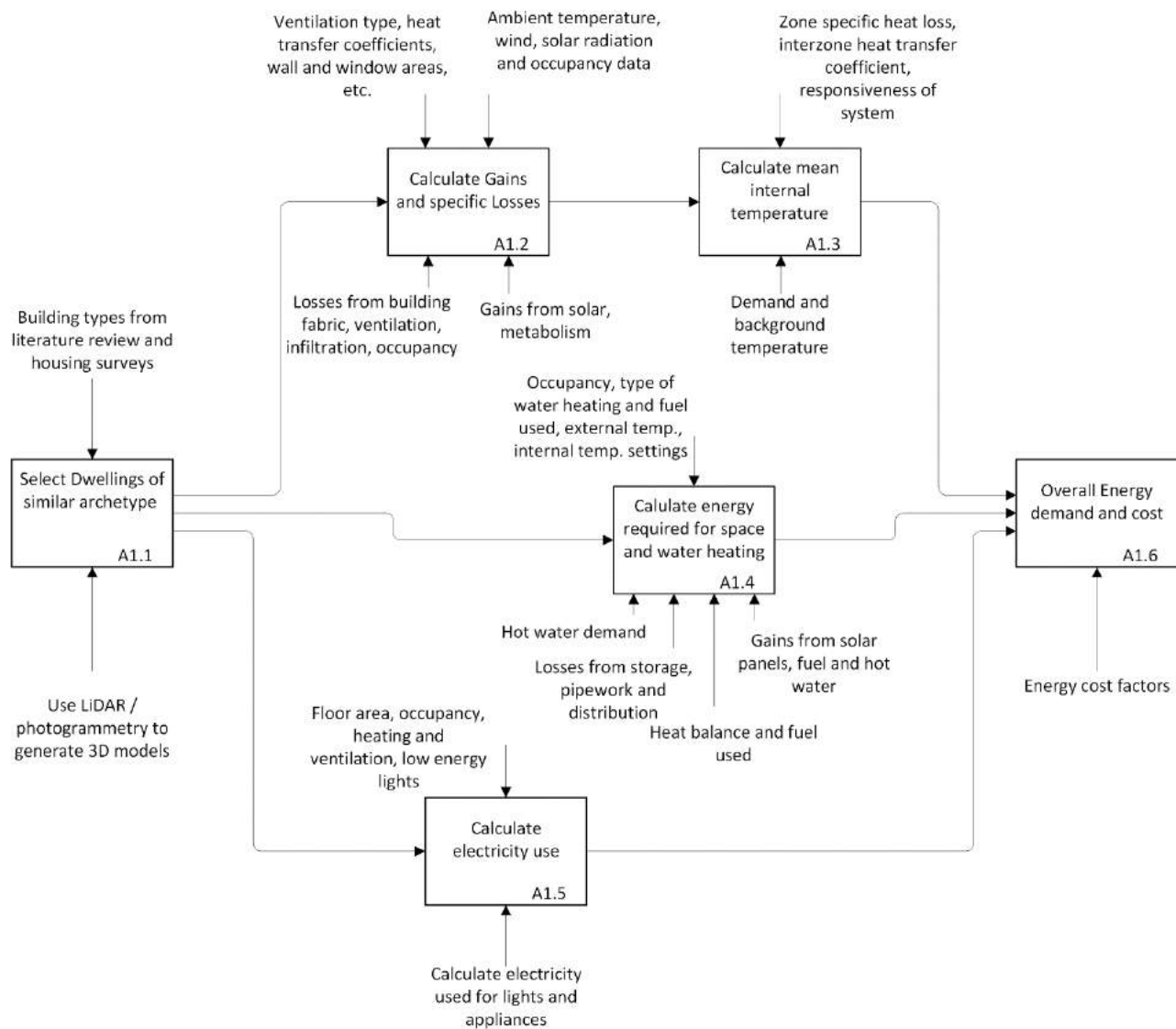


Figure 24 Energy performance assessment based on SEMANCO project – adapted from Dawood et al. (2017)

5.2.1 Comparison of data/results with current industry standard procedures

The data captured using the LiDAR and photogrammetry methods will provide the inputs for the determination of energy demand based on the Standard Assessment Procedure (SAP).

The Standard Assessment Procedure (SAP) is the methodology used by the UK Government to assess and compare the energy and environmental performance of dwellings. SAP was developed by the Building Research Establishment (BRE) and is based on the BRE Domestic Energy Model (BREDEM), which provides a framework for calculating the energy consumption of dwellings (BEIS 2014).

The SAP methodology provides an assessment of how much energy a dwelling will consume, when delivering a defined level of comfort and service provision. The

assessment is based on standardised assumptions for occupancy and behaviour. SAP quantifies a dwelling's performance in terms of (BEIS 2014):

- energy use per unit floor area,
- fuel-cost-based energy efficiency rating (the SAP Rating),
- emissions of CO₂ (the Environmental Impact Rating),
- estimate of appliance energy use,
- potential for overheating in summer and the resultant cooling load.

These indicators of performance are based on estimates of annual energy consumption for the provision of space heating, domestic hot water, lighting and ventilation.

Reduced Data SAP (RdSAP) was introduced as a simplified method of assessing the energy performance of existing dwellings, and will be used as the energy assessment method for comparison. RdSAP is used to produce Energy Performance Certificates (EPC) for existing dwellings in the UK (BEIS 2014).

LiDAR and photogrammetry data provide key geometry values that need to be considered as input measurements into the RdSAP calculation process. The input geometry is (a) the shape of the property; measured as the gross external footprint of the individual dwelling unit; and (b) the height of the property (Dawood et al. 2017).

In addition to the geometric data from LiDAR and photogrammetry, other data is needed in order to conduct accurate neighbourhood energy performance evaluation. This will include the use of published databases such as Homes Energy Efficiency Database (HEED), household surveys such as English House Condition Survey (EHCS), census and the Office of National Statistics (ONS) as data sources for input for the core SAP calculation engine as detailed in Mhalas et al. (2014).

The use of these input parameters in RdSAP assessment provides an accurate calculation of heat-loss parameters around the extent of internal heated living space relative to the exposed surface areas including the ground floor, external walls and roof (Dawood et al. 2017).

The application of the ROI methodology to thermal images detailed in section 5.1 will provide a range of temperature values for individual building features such as walls, windows, roofs and HVAC assets. Using this methodology it is possible to isolate features from the building envelope such as the external walls and roof of the building

and estimate their U values (i.e. overall heat transfer coefficient (W/m²K)), as well as the transmission heat losses (Fokaides & Kalogirou, 2011; González-Aguilera et al. 2013). The estimated transmission heat losses will be considered as an input to the estimation of energy demand, and will be used to estimate demand-side improvement potential, which will inform the DR potential estimation process. Taking into account the uncertainties associated with the determination of energy demand based on thermal images (González-Aguilera et al. 2013), Demand-side improvement potential will be provided in a range of values, similar to EPC certificates (Fig. 25). Analysis of thermal imagery data will also provide information about users/customers behaviour, which will be considered in the determination of demand-side improvement potential, as well as in the determination of adequate DR strategies. The results will be compared to the results obtained considering theoretical values, as well as with existing meter data, in order to evaluate the accuracy and feasibility of the proposed experimental approach.

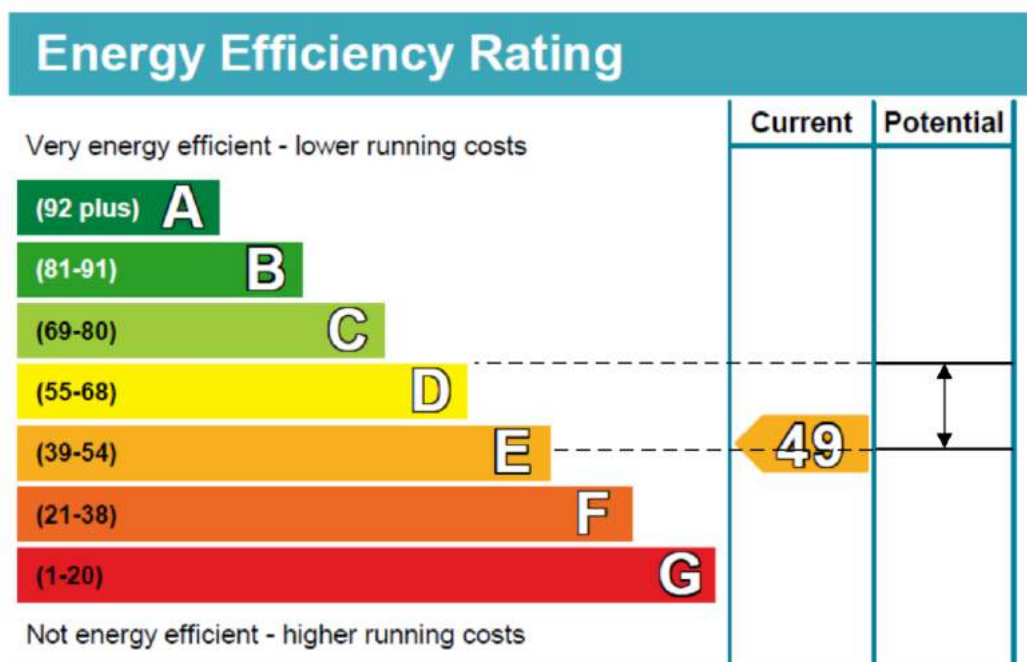


Figure 25 Determination of Energy demand reduction potential using EPC – adapted from OFGEM (2017)

6 Conclusions

This report serves to investigate the process of utilising aerial surveying techniques on buildings with the aim of creating geometrically accurate models of buildings with thermal data and region of interest DR asset detection functionality. This report gathers and outlines the methods, techniques and development work that will be used for the activities within task T3.4, leading into the final outcomes of D3.8. This document explores the technical development, software research and decisions, aerial survey techniques and data analysis techniques which are required to fulfil the required outcomes of this task.

Chapter 2 investigates the decision-making process involved in choosing the aircraft used, and the payload considerations and development efforts involved. Due to the heavy nature of the payloads that need to be carried, a DJI Matrice M210 was chosen to allow stable carrying of heavy payloads while achieving excellent flight time capability. A suitable thermal camera, the Zenmuse XT2 was chosen and the LiDAR unit used by the partner Teesside University was adapted for use as an aerial payload.

Chapter 3 investigates the software used to interface with the LiDAR, perform thermography and photogrammetry, as well as any alternative considerations. There are many options which have been discovered for interfacing with the LiDAR, however at this time it has been determined that the most efficient way of doing so is to utilise the software provided by Velodyne, Veloview, to perform packet capture onboard the aircraft for subsequent processing on the ground. Regarding the thermography aspect, the manufacturer of the sensor inside of the Zenmuse XT2, FLIR, provides a software called FLIR tools with a great deal of functionality including the ability to convert images directly to CSV matrices of temperature values for each pixel of the sensor. This has been deemed to be the most suitable method of converting this data into a useful format for further processing. Regarding photogrammetry the software suite chosen was Pix4D, which includes functionality for establishing the flight path, executing the scanning process and then processing the resulting images. Further investigations are still ongoing regarding potentially superior options such as videogrammetry to increase the number of model data points available compared to photogrammetry techniques. Chapter 4 investigates the planning process for performing the aerial survey activities, including legal and regulatory considerations, site suitability and scanning site techniques. This work performed in this chapter discovered that despite the site which

was initially intended to be used for this task being very attractive due to its high data availability and comprehensive climate control systems, it was deemed to be unsuitable as a pilot site for this task as it is located in the financial sector of the city of London, which is designated as a flight restricted zone. This would make performing the aerial survey extremely difficult, so a new location was chosen. The replacement location selected was the Ernest Dence estate in Greenwich, London. This site, while having a lower data availability and being slightly less interesting, is outside of the financial district and far enough away from airports to not be within a flight restricted zone. Legal and regulatory factors pertaining to such aerial survey activities are investigated and reported, following on from the efforts performed in D2.3, eDREAM Standardization Report and Regulatory Roadmap to ensure that all actions performed adhere to local legislation. Finally, the considerations and route planning process are investigated, with different scanning techniques assessed and recommendations are made. Pix4D will be used to implement optimal route planning, using a combination of Double Grid, Circular and Free Flight during the testing phase. Adjustments to the route planning strategy may be made at a later date once more information is gained about specific characteristics of the pilot site are learned, improving the scanning procedure as an iterative process.

Finally chapter 5 investigates and specifies the methods that will be used for building thermal loss and ROI analysis to provide automated thermal performance analysis and DR asset detection and analysis. These indicators are then used to provide mathematically modelled characteristics of a buildings energy consumption, production and DR flexibility. Finally a methodology is established to compare the results obtained with industry standard procedures for assessment and validation.

References

- L.C.Chen et al. "Deeplab: Semantic image segmentation with deep convolutional nets, atrous convolution, and fully connected CRFs" IEEE transactions on pattern analysis and machine intelligence 40.4, pp.834-848, 2018.
- BEIS (2014) Standard Assessment Procedure Guidance on how buildings will be SAP energy assessed under the Green Deal and on recent changes to incentivise low carbon developments. Available at: <https://www.gov.uk/guidance/standard-assessment-procedure> Accessed on: 16th May 2019
- Dawood, N., Dawood, H., Rodriguez-Trejo, S. et al. Vis. in Eng. (2017) 5: 22. <https://doi.org/10.1186/s40327-017-0060-3>
- ESRI (2018) Introduction to ortho mapping. Available at: <https://pro.arcgis.com/en/pro-app/help/data/imagery/introduction-to-ortho-mapping.htm>) Accessed on: 14th May 2019
- Gharibi, H.; Habib, A. (2018) True Orthophoto Generation from Aerial Frame Images and LiDAR Data: An Update. Remote Sens. 2018, 10, 581
- D. González-Aguilera, S. Lagüela, P. Rodríguez-González, D. Hernández-López (2013), Image-based thermographic modeling for assessing energy efficiency of buildings façades, Energy and Buildings, Volume 65, 2013, Pages 29-36, ISSN 0378-7788, <https://doi.org/10.1016/j.enbuild.2013.05.040>.
- Ham, Y. & Golparvar-Fard, M., 2012. Rapid 3D Energy Modeling for Retrofit Analysis of Existing Buildings Using Thermal and Digital Imagery. LiDAR Magazine, Vol. 2, No. 4
- K.He et al. "Mask R-CNN", IEEE International Conference on Computer Vision (ICCV), 2017.
- A. Mhalas ; T. Crosbie ; N. Dawood ; and M. Kassem (2014), Assessing Energy Improvement Potential from Efficiency and Renewable Interventions at Neighborhood Level, Computing in Civil and Building Engineering (2014) . 2014
- OFGEM (2017), Frequently Asked Questions – Domestic Renewable Heat Incentive (RHI) FAQs about Energy Performance Certificates (EPCs). Available at: https://www.ofgem.gov.uk/system/files/docs/2017/11/drhi_faqs_about_epcs_v2_0_29_nov_2017.pdf Accessed on: 28th May 2019
- Paris A. Fokaides, Soteris A. Kalogirou (2011), Application of infrared thermography for the determination of the overall heat transfer coefficient (U-Value) in building envelopes, Applied Energy, Volume 88, Issue 12, 2011, Pages 4358-4365, ISSN 0306-2619, <https://doi.org/10.1016/j.apenergy.2011.05.014>.
- Patacas J., Dawood H., and Dawood N. (2018) Visualisation of industrial facilities for operations and decommissioning, Proceedings of the 18th Int. Conf. on Construction Applications of Virtual Reality (CONVR) 22 to 23 Nov 2018, Auckland, New Zealand
- T.Rakha and A.Gorodetsky. "Review of Unmanned Aerial System (UAS) applications in the built environment: Towards automated building inspection procedures using drones." Automation in Construction 93, pp.252-264, 2018.